Mechanisms for the Development of Unstable Dimension Variability and the Breakdown of Shadowing in Coupled Chaotic Systems

Ernest Barreto* and Paul So

Department of Physics and Astronomy and the Krasnow Institute for Advanced Study, George Mason University, Fairfax, Virginia 22030

(Received 30 March 2000)

A chaotic attractor containing unstable periodic orbits with different numbers of unstable directions is said to exhibit unstable dimension variability (UDV). We present general mechanisms for the progressive development of UDV in uni- and bidirectionally coupled systems of chaotic elements. Our results are applicable to systems of dissimilar elements without invariant manifolds. We also quantify the severity of UDV to identify coupling ranges where the shadowability and modelability of such systems are significantly compromised.

PACS numbers: 05.45.Xt, 05.45.Pq, 05.45.Ra, 87.10.+e

The phenomenon known as unstable dimension variability (UDV) refers to the presence of unstable periodic orbits (UPOs) with different numbers of unstable directions embedded within a chaotic attractor. Although first described long ago [1], interest in UDV and its consequences has grown recently [2–8], especially since it was observed in a physically motivated model [9]. Severe UDV has profound implications. The authors of Ref. [2] showed that the presence of a Lyapunov exponent that fluctuates about zero, a situation which arises in systems with a high degree of UDV, causes severe shadowing difficulties. This means that the significance of numerically generated trajectories is called into question: a long numerical trajectory may not correspond to *any* mathematically true solution of the underlying equations. More recently, it has been argued that systems that exhibit UDV may be, in principle, *deterministically unmodelable* [3]. Thus, it is very important to have an understanding of what conditions lead to the occurrence of UDV, and how UDV develops as these conditions are approached.

In this paper we present a detailed analysis of the mechanisms that lead to the development of UDV as synchronized coupled chaotic systems desynchronize. In addition, we quantify the degree of UDV as a function of coupling and find significant ranges of coupling where UDV is so severe that even very short numerically generated trajectories are suspect. Our results are novel in that they are applicable to coupled systems that do not possess inherent symmetries and/or synchronization manifolds, such as coupled systems with *dissimilar* elements. We draw particular attention to this case, since it represents almost every experimental situation of interest: in practice, it is very difficult to prepare sets of truly identical oscillators in physical experiments, and, in biological systems, natural oscillators occur with considerable variability (for example, note the large variety of different neurons in the brain).

We begin with a "subsystem" decomposition of a general unidirectionally coupled system of chaotic maps (we discuss the bidirectionally coupled case subsequently):

$$\begin{cases} x \to f(x) \\ y \to G(x, y; c)\,. \end{cases} \tag{1a}$$

We assume that at $c = 1$ the x and y dynamics are in generalized synchrony [10], and that at $c = 0$ the x and y dynamics are chaotic and independent of one another. f and G may be of any dimension. For ease of presentation, we use the simplest case

$$G(x, y; c) = cf(x) + (1 - c)g(y) \tag{1b}$$

and take f and g to be quadratic maps with different parameters in our discussion below. Our arguments, however, are not specific to these choices.

The subsystem decomposition of Eq. (1) is defined as follows [11]. First, enumerate the periodic orbits of f (the driver), assigning each an index $i = 1, 2, \ldots$. Then subsystem S_i is given by Eq. (1), but with the driver dynamics, $f(x)$, locked on orbit i. We are interested in investigating the dynamics of individual subsystems. Note that because the driver is chaotic, an x trajectory will come arbitrarily close to (and spend an arbitrarily long time near) any of the unstable periodic orbits embedded within its attractor. Thus, subsystem S_i contains the dynamics that the full-system trajectory experiences during close approaches to orbit i.

As the coupling c is varied, each subsystem S_i exhibits an independent bifurcation structure in its y component. Each of these begins at $c = 1$ with x and y synchronized at the driving periodic orbit and progresses (via period-doubling sequences, etc.) to the chaotic dynamics of g at $c = 0$. To illustrate, let $f(x) = 1.9 - x^2$ and $g(y) = 1.6 - y^2$, both of which are chaotic. The top panels in Fig. 1 show partial bifurcation diagrams of subsystems that are driven by a period-3 and a period-4 driver. A vertical line is superimposed on each figure at $c = 0.16$. At this particular coupling value, the period-3 subsystem (a) exhibits an attracting periodic orbit (of period 9), while the period-4 subsystem (b) exhibits chaos. The bottom

 0031-9007/00/85(12)/2490(4)$15.00

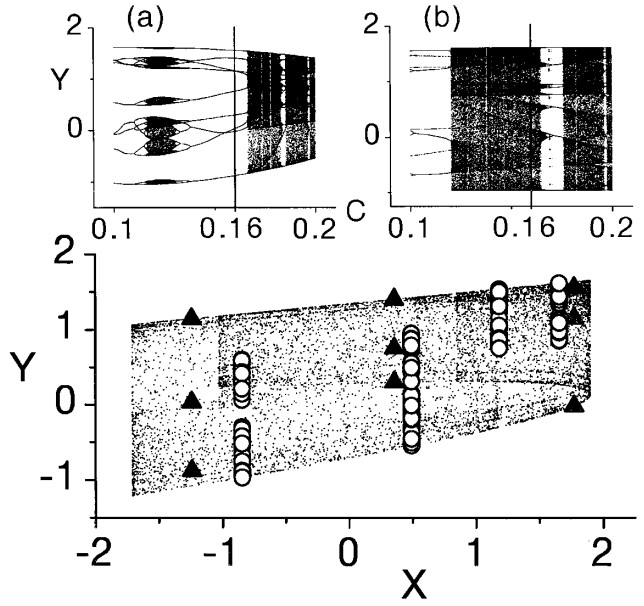

FIG. 1. Unstable dimension variability for Eq. (1) with $f(x) = 1.9 - x^2$ and $g(y) = 1.6 - y^2$. The top panels show partial bifurcation diagrams of subsystems with (a) a period-3 and (b) a period-4 driver; the vertical lines are placed at $c = 0.16$. The bottom panel shows the overall attractor at this coupling value with the subsystem dynamics superimposed. Triangles denote a period-9 saddle [attracting orbit shown in (a)]; circles denote an infinite number of repellers [chaotic orbit shown in (b)].

panel shows the attractor for the overall coupled system. The asymptotic trajectories of the period-3 and period-4 subsystems are superimposed with triangles and circles, respectively.

We now argue that UDV is present in the example considered above, with $c = 0.16$. The period-3 subsystem is a periodically forced one-dimensional quadratic map in the y variable. For $c = 0.16$, it has an attracting period-9 orbit q whose stable set is an interval I_q in y (approximately $[-2, 2]$; compare scales in Fig. 1). Viewed as an orbit of the original coupled map, Eq. (1), q is a *saddle* UPO. In particular, it has one stable direction along y, since its corresponding subsystem is attracting, and one unstable direction (with a nonzero projection along x), since f is chaotic. Correspondingly, the period-4 subsystem with $c = 0.16$ has a one-band chaotic attractor A in y whose stable set I_A is also an interval in y (again, approximately $[-2, 2]$). From similar arguments we conclude that A is a chaotic saddle of Eq. (1) and thus contains a dense set of *repellers* with two unstable directions (this is the one-dimensional version of the situation described in [7]).

Viewed in the full space of Eq. (1), the stable sets of q and A take on an additional complication. That is, the stable set of q (A) is the direct product of the set of preimages of the driving period-3 (4) orbit and the union of the appropriate preimages of I_q (I_A) [12]. Both these stable sets intersect the full attractor (compare I_q and I_A to Fig. 1), and thus both q (saddle UPO) and A (containing repeller UPOs) are embedded within it.

Finally, we argue that q and A are recurrently connected in the sense of Ref. [7]. From the previous discussion, the stable sets of q and A are at least one dimensional since they contain a collection of intervals. Furthermore, the unstable sets of q and A are also at least one dimensional, as can be seen by considering the evolution of a small interval in x centered around either q or a repeller within A. Because two lines generically intersect in two dimensions, we conclude that the stable set of q intersects the unstable set of A and that the unstable set of q intersects the stable set of A. These intersections are typically not destroyed by small perturbations. Thus we expect trajectories to visit both q and A recurrently.

These arguments establish UDV for Eq. (1) with $c = 0.16$. Other subsystems can be used in a similar manner to establish the simultaneous presence of additional saddle and repeller UPOs in the attractor; see Table I. We confirm the presence of UDV in the full two-dimensional system by observing that the second largest finite-time Lyapunov exponent fluctuates about zero (inset in Fig. 2).

We now use the subsystem decomposition of Eq. (1) to elucidate two distinct mechanisms for the development of UDV as the coupling is varied from 1 to 0 and the system desynchronizes. According to the subsystem decomposition, we think of each subsystem as a separate chaotic system with its own bifurcation structure, but with all subsystems sharing the coupling c as the bifurcation parameter. For $c = 1$, the overall dynamics is (by construction) attracted to the diagonal $x = y$, and each subsystem S_i collapses onto an orbit of period equal to that of its driver orbit. As c is decreased, a bifurcation analogous to the bubbling transition occurs [13]. At this critical value of coupling, one particular subsystem (typically with a low-period driver) undergoes a bifurcation which converts the previously stable orbit to an unstable one. When viewed as a UPO of the combined system, this orbit is unstable in both the x and y directions. This is the first repeller UPO to appear, and this bubblinglike transition marks the first appearance of UDV.

As c is further decreased, other subsystems undergo similar bifurcations that create additional repellers. Meanwhile, the unbifurcated subsystems contribute saddle

TABLE I. Largest Lyapunov exponents of several subsystems with drivers of periods 1–10 for $f(x) = 1.9 - x^2$, $g(y) = 1.6 - y^2$, and $c = 0.16$. A negative Lyapunov exponent implies the presence of a saddle UPO in the attractor; a positive exponent implies the presence of an infinite number of repeller UPOs.

Driver period	Lyapunov exponent	Driver period	Lyapunov exponent
1	−0.038	6	−0.394, **0.171**
2	**0.185**	7	−0.145, **0.176**
3	−0.363	8	−0.306, **0.143**
4	**0.167**	9	−0.141, **0.103**
5	−0.014, **0.159**	10	−0.130, **0.187**

UPOs to the overall attractor. This is the first mechanism for the development of UDV. If the coupled system possesses an inherent symmetry, as when the coupled elements are identical, all of these orbits reside on an invariant synchronization manifold that contains the overall attractor; this is essentially the case studied in Ref. [3]. Our subsystem analysis, however, is not restricted to systems with such symmetries. More importantly, we argue below that the dominant contribution to severe UDV comes from the set of new orbits created as the various subsystems bifurcate.

As c is further decreased, still more subsystems bifurcate as described above. Meanwhile, a second parallel mechanism proceeds: the new orbits that are created as each individual subsystem bifurcates (usually via period doubling) undergo cascades of period doublings to chaos, apparently independently of one another. This process creates a huge number of new saddle and repeller UPOs in the overall system. We call the set of new orbits created in this way the *emergent set*. For $f = g$, these orbits reside outside the attractor until the blowout bifurcation [14]. However, in the more general case $f \neq g$, the destruction of the synchronization manifold (present only at $c = 1$) leads to the incorporation of most of the emergent set into the attractor [11]. Thus, for $f \neq g$, the combination of the two mechanisms outlined above leads to a dramatic increase in UDV. We believe that UDV is most severe once the system has lost topological coherence [11] and the emergent set dominates the overall dynamics.

We conjecture that there is a set C of positive Lebesgue measure consisting of coupling values c at which some subsystems exhibit attracting periodic orbits while *simultaneously* other subsystems exhibit chaos. At such values of $c \in C$, one can deduce by the arguments above that the attractor of the coupled system exhibits UDV. This implies that UDV can and will be encountered *in practice* when studying generic coupled chaotic systems, and thus the potential for severe shadowing and/or modeling breakdown is an important consideration for researchers investigating such systems.

It is reasonable to expect that C has positive measure in light of the results of Refs. [15–17]. Jacobson [15] proved that in the quadratic family, the set of parameter values that gives rise to chaos has positive measure. Thus, if we assume that at a particular fixed value of c, the various subsystems are in some sense at random positions in each of their respective bifurcation diagrams (as numerical investigations suggest), then there is a positive probability that at least some subsystems exhibit chaos and thus contribute repellers to the overall attractor. On the other hand, Graczyk and Świątek [16] proved, also for the quadratic family, that windows (i.e., parameter intervals that yield periodic behavior) occur densely in the parameter space. Thus it is also reasonable to expect that for the same fixed value of c, at least some subsystems exhibit attracting periodic orbits and therefore contribute saddles to the overall attractor. It is generally believed that the results of Refs. [15,16] carry over to higher dimensional situations in sufficiently high-dimensional parameter spaces [17].

Our arguments in this work do not rely on any specific features of f and G, other than that they are chaotic and that they desynchronize as the coupling between them is reduced to zero. Thus, the mechanisms for the creation of UDV in coupled systems described here is very general. In the case of *bidirectionally* coupled chaotic systems, distinct subsystems cannot be easily defined. Nevertheless, mechanisms similar to those described here can be observed [18]. More specifically, as a bidirectionally coupled system desynchronizes, the unstable periodic orbits embedded in the synchronized chaotic attractor lose transverse stability, typically via period-doubling bifurcations (mechanism 1); simultaneously, the new orbits created in this fashion undergo their own period-doubling cascades to chaos (mechanism 2). In contrast to the unidirectional case, these bifurcation sequences do not proceed independently. Instead, they interfere with each other and can lead to attractor crises [19] in the overall system. For example, such crises may lead to the destruction of the chaotic attractor and its replacement by an attracting periodic orbit. (In this case, however, a nonattracting chaotic set would remain containing UDV.)

In the following, we quantify the degree of UDV and measure its evolution as a function of coupling. We consider both system (1) and a bidirectionally coupled case. For the latter, we use $x \to (1 - c)f(x) + cg(y)$ and take y as in Eq. (1b). To quantify UDV, a *contrast measure,* defined for orbits of a given fixed period, has been proposed [5]. Here, we use the methods of Ref. [4] to estimate the expected shadowing time. In effect, this takes UPOs of all periods into account at once. More importantly, the expected shadowing time is a physically relevant quantity that estimates the limitations of computer-based calculations.

The authors of Ref. [4] use a random walk approach to model the distribution of pointwise shadowing distances, i.e., the pointwise distances from a numerically generated trajectory to its corresponding mathematically true "shadowing" orbit. The random walk, which includes a drift towards a reflecting barrier at the noise level, draws its parameters from the distribution of the finite-time Lyapunov exponent closest to zero. This is reasonable because the pointwise shadowing distance grows precisely when trajectories alternate between regions with different numbers of unstable directions. As the degree of UDV increases, such alternations occur more frequently. The expected shadowing time is calculated as the first-passage time for the shadowing distance to grow to the attractor size. In particular, the expected shadowing time may be estimated as 10^{pE}, where p is the number of digits of accuracy in the numerical computation and $E = \frac{2|m|}{\sigma^2}$. Here, m and σ^2 are the mean and variance of the distribution of the finite-time Lyapunov exponent closest to zero [20].

Figure 2 shows the exponent E versus coupling for our two example systems, with $f(x) = 1.9 - x^2$ and $g(y) = 1.6 - y^2$. The horizontal lines correspond to expected shadowing times of 10^6 and 10^3 iterations, assuming a calculational accuracy of 10^{-16}. The solid curve represents the unidirectionally coupled case; the dotted curve with circles is the bidirectionally coupled data. In both cases, there is a significant range of coupling for which E is very small, thus indicating severe UDV and very short shadowing times. E is calculated using 10 000 time-50 Lyapunov exponents at each value of coupling; error bars indicate the standard deviation of 20 measurements. The arrows indicate ranges of coupling values over which E is not graphed for the bidirectional case: within most of this range the system exhibits stable periodic behavior, and at the small-coupling end of the left arrow, these orbits period double into a small two-piece chaotic attractor which explodes into the full attractor just below $c = 0.09$. The shaded region corresponds to shadowing times shorter than 50 iterations.

Finally, numerically generated trajectories of systems with very short shadowing times may visit regions of the phase space with a frequency that is different from the system's true natural measure. Thus, infinite-time dynamical averages such as Lyapunov exponents, dimensions, and entropies may not be accurate in such cases. To our knowledge there are no quantitative results linking expected errors for infinite-time averages to estimated shadowing times (related work is reported in [6]). On the other hand, time-T averages for T less than the expected shadowing time (such as E values falling outside of the shaded box in Fig. 2) should be reliable.

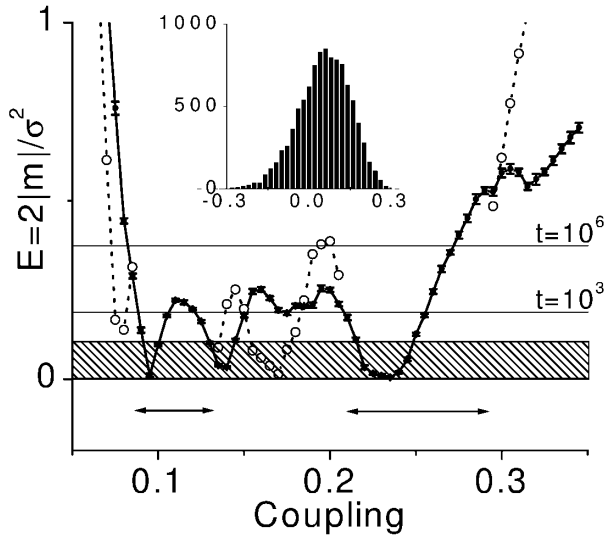

FIG. 2. Shadowing time exponent E versus coupling (inset: distribution of the time-50 Lyapunov exponent closest to zero for $c = 0.16$, unidirectional case). The solid curve represents the unidirectionally coupled case; the dotted curve with circles is the bidirectionally coupled data. Horizontal lines indicate expected shadowing times of 10^6 and 10^3 iterations, assuming a calculational precision of 10^{-16}. Arrows indicate ranges of coupling values over which E is not graphed for the bidirectional case; see text.

We thank Mitrajit Dutta, Celso Grebogi, and Tim Sauer for helpful discussions and encouragement. This work was supported by the NSF (IBN 9727739); P. S. was also supported in part by the NIH (2R01MH50006).

*E-mail address: ebarreto@gmu.edu
See also http://complex.gmu.edu

[1] R. Abraham and S. Smale, Proc. Symp. Pure Math. **14**, 5 (1970).
[2] S. Dawson, C. Grebogi, T. Sauer, and J. A. Yorke, Phys. Rev. Lett. **73**, 1927 (1994).
[3] Y.-C. Lai and C. Grebogi, Phys. Rev. Lett. **82**, 4803 (1999); Y.-C. Lai, D. Lerner, K. Williams, and C. Grebogi, Phys. Rev. E **60**, 5445 (1999).
[4] T. Sauer, C. Grebogi, and J. A. Yorke, Phys. Rev. Lett. **79**, 59 (1997).
[5] Y.-C. Lai, Phys. Rev. E **59**, R3807 (1999).
[6] Y.-C. Lai, C. Grebogi, and J. Kurths, Phys. Rev. E **59**, 2907 (1999).
[7] S. P. Dawson, Phys. Rev. Lett. **76**, 4348 (1996); P. Moresco and S. P. Dawson, Phys. Rev. E **55**, 5350 (1997).
[8] E. J. Kostelich, I. Kan, C. Grebogi, E. Ott, and J. A. Yorke, Physica (Amsterdam) **109D**, 81 (1997).
[9] F. J. Romeiras, C. Grebogi, E. Ott, and W. P. Dayawansa, Physica (Amsterdam) **58D**, 165 (1992).
[10] V. S. Afraimovich, N. N. Verichev, and M. I. Ravinovich, Izv. Vyssh. Uchebn. Zaved. Radiofiz. **29**, 1050 (1986) [Radiophys. Quantum Electron. **29**, 795 (1986)]; N. F. Rulkov, M. M. Sushchik, L. S. Tsimring, and H. D. I. Abarbanel, Phys. Rev. E **51**, 980 (1995); L. Kocarev and U. Parlitz, Phys. Rev. Lett. **76**, 1816 (1996).
[11] E. Barreto, P. So, B. J. Gluckman, and S. J. Schiff, Phys. Rev. Lett. **84**, 1689 (2000).
[12] The preimages of I_q (or I_A) must be defined in terms of a sequence of maps $\{g_j\}$, where g_0 is the period-3 (4) subsystem and g_j is the response system driven by the jth preimage of the orbit that drives g_0.
[13] For $f = g$, this transition is identical to the bubbling transition. See P. Ashwin, J. Buescu, and I. Stewart, Phys. Lett. A **193**, 126 (1994); S. C. Venkataramani, B. R. Hunt, and E. Ott, Phys. Rev. E **54**, 1346 (1996). For $f \neq g$, this bubblinglike transition is described in [11].
[14] At the blowout bifurcation, the synchronization manifold becomes repelling, on average. See E. Ott and J. C. Sommerer, Phys. Lett. A **188**, 39 (1994).
[15] M. V. Jacobson, Commun. Math. Phys. **81**, 39 (1981).
[16] J. Graczyk and G. Świątek, Ann. Math **146**, 1 (1997).
[17] E. Barreto, B. R. Hunt, C. Grebogi, and J. A. Yorke, Phys. Rev. Lett. **78**, 4561 (1997).
[18] V. Astakhov, A. Shabunin, T. Kapitaniak, and V. Anishchenko, Phys. Rev. Lett. **79**, 1014 (1997).
[19] E. Ott, *Chaos in Dynamical Systems* (Cambridge University Press, Cambridge, England, 1993).
[20] The variance σ^2 is calculated using time-T Lyapunov exponents as $T\sigma_T^2$; we use $T = 50$. See Ref. [4].